ARMY RESEARCH LABORATORY

Characterization of Acoustic Ground Impedance at Blossom Point Research Facility

by W. C. Kirkpatrick Alberts, II, Mark A. Coleman, and John M. Noble

ARL-TR-5352   **September 2010**

NOTICES

Disclaimers

Army Research Laboratory

Adelphi, MD 20783-1197

ARL-TR-5352 **September 2010**

Characterization of Acoustic Ground Impedance at Blossom Point Research Facility

W. C. Kirkpatrick Alberts, II, Mark A. Coleman, and John M. Noble
Computational and Information Sciences Directorate, ARL

REPORT DOCUMENTATION PAGE

1. REPORT DATE *(DD-MM-YYYY)*	2. REPORT TYPE	3. DATES COVERED *(From - To)*
September 2010		

4. TITLE AND SUBTITLE	5a. CONTRACT NUMBER
Characterization of Acoustic Ground Impedance at Blossom Point Research Facility	
	5b. GRANT NUMBER
	5c. PROGRAM ELEMENT NUMBER

6. AUTHOR(S)	5d. PROJECT NUMBER
W. C. Kirkpatrick Alberts, II, Mark A. Coleman, and John M. Noble	
	5e. TASK NUMBER
	5f. WORK UNIT NUMBER

7. PERFORMING ORGANIZATION NAME(S) AND ADDRESS(ES)	8. PERFORMING ORGANIZATION REPORT NUMBER
U.S. Army Research Laboratory ATTN: RDRL-CIE-S 2800 Powder Mill Road Adelphi, MD 20783-1197	ARL-TR-5352

9. SPONSORING/MONITORING AGENCY NAME(S) AND ADDRESS(ES)	10. SPONSOR/MONITOR'S ACRONYM(S)
	11. SPONSOR/MONITOR'S REPORT NUMBER(S)

12. DISTRIBUTION/AVAILABILITY STATEMENT

Approved for public release; distribution unlimited.

13. SUPPLEMENTARY NOTES

14. ABSTRACT

The propagation of sound in the atmosphere is greatly influenced by the acoustic impedance of the ground surface. As part of a recent urban acoustics study (Alberts, et al. *J. Acoust. Soc. Am. 2008*, *124* (2)), and as part of the revision of American National Standards Institute (ANSI) standard S1:18-1999: Template Method for Ground Impedance, the ground impedance was measured at three sites at the U.S. Army Research Laboratory's (ARL) Blossom Point Research Facility: a grass field, an asphalt road, and a gravel road. This report describes the measurements and results at each of the three sites.

15. SUBJECT TERMS

Acoustic ground impedance

16. SECURITY CLASSIFICATION OF:			17. LIMITATION OF ABSTRACT	18. NUMBER OF PAGES	19a. NAME OF RESPONSIBLE PERSON
			UU	24	W. C. Kirkpatrick Alberts, II
a. REPORT	b. ABSTRACT	c. THIS PAGE			19b. TELEPHONE NUMBER *(Include area code)*
Unclassified	Unclassified	Unclassified			(301) 394-2121

Contents

List of Figures

List of Tables

1. Introduction

Sound propagating in the atmosphere is affected by many processes (wind, turbulence, terrain shape, etc.) that change the magnitude and phase of a source's signal as it travels to a receiver. Amongst these processes, the impedance of the ground is often important (*1*). The ground varies from acoustically hard surfaces, such as asphalt and hard packed soil, to acoustically soft surfaces, such as snow (*2, 3*). These extremes in impedance have vastly different effects on the amplitude and phase of a ground-reflected wave. Thus, knowledge of the acoustic impedance of the ground is important in obtaining an overall picture of the environment through which sound is propagating.

As part of an ongoing urban acoustics study (*4*), the ground impedance at the Blossom Point Research Facility (BPRF) has been characterized using the method prescribed in American National Standards Institute (ANSI) *S1.18-1999: Template Method for Ground Impedance* (*5*), which will be henceforth referred to here as the Template Method. Several methods exist for the measurement/deduction of the specific acoustic ground impedance (*6–8*), the ratio of the surface pressure to the average particle velocity of the fluid directed at the ground surface, but the Template Method was chosen for its ease of use (*5, 9*).

The following section describes the experimental configurations used over three surfaces at BPRF. Section 3 presents level difference spectra for each of the surfaces superimposed on calculated level difference spectra. In addition, the third section offers qualitative comparisons between the measurements and calculations. Concluding remarks appear in the fourth section.

2. Experimental Configuration

In the Template Method, a point source is positioned a short distance from two microphones separated in height perpendicularly above the ground. This allows the difference in sound level between the microphones to be measured. Using this level difference spectrum, the acoustic impedance of the ground can be deduced by comparing the measurement with calculated level differences. The Template Method describes three different geometries (A, B, and C), listed in table 1, that are used to measure level difference spectra above ground surfaces. Figure 1 shows a drawing of the experimental configuration. Each geometry has been designated in the Template Method for its potential performance on a given soil type: geometry A tends to cover the largest frequency range; geometry B may produce best results over hard grounds at frequencies greater than 1 kHz; and geometry C is, perhaps, best used over soft grounds for frequencies below 1 kHz. All geometries were used during experiments over grass and asphalt. Only geometries A and B were used over gravel. The lack of geometry C in the gravel

measurement is due to the revised standard in which geometry C has been removed in favor of the more general geometries A and B. ARL provided a worked example of the revised Template Method over gravel to the ANSI ground impedance measurement working group.

Table 1. Geometries specified in the Template Method (*2*).

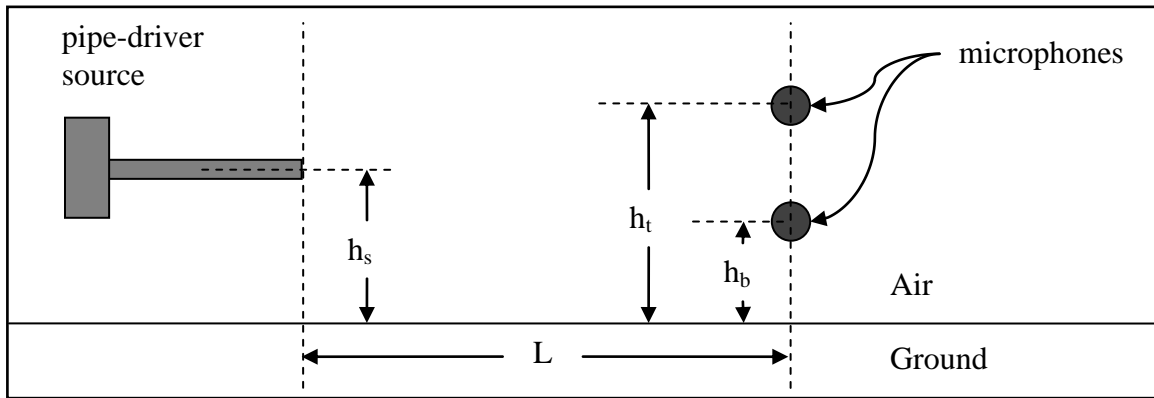| Geometry	Source Height: h_s (cm)	Top Microphone Height: h_t (cm)	Bottom Microphone Height: h_b (cm)	Source/Microphone Horizontal Separation (m)
A	32.5	46	23	1.75
B	20	20	5	1
C	40	40	5	1

Figure 1. Drawing of experimental configuration.

The source used for this work was a pressure driver coupled to a pipe of 0.5 m length and 3.175 cm diameter. This pipe-driver combination can be approximated as a point source to a frequency of nearly 2.7 kHz. However, because the pipe is 50 cm in length, there is potential for reflections from the face of the driver at the highest operating frequencies. These reflections tend to degrade the point-source performance of the pipe-driver system and, thus, alter the experimental results when they are compared to level differences calculated assuming spherical waves. Microphones used were half-inch pressure field microphones. The source waveform used in all instances was white noise that was band-limited from 150 Hz to 2.7 kHz. Microphone data were collected using a data acquisition computer sampling at 10 kilo-samples per second. Recorded microphone data were also filtered from 150 Hz to 2.7 kHz. During grassland and asphalt experiments, 60 s of data were collected for each of five sub-sites on each surface. During gravel experiments 30 s of data were collected for each of four sub-sites. In post-processing, recorded data were separated into one-second blocks with one third overlap between blocks. Each block was Hanning windowed, Fourier transformed, and all blocks were magnitude averaged for each ground type. During each experiment wind speeds and air temperatures were monitored; wind speeds remained less than the 2.5 m/s called for in the Template Method and measured temperatures were used in calculations during the analysis of the results. Temperatures during the measurements over grass and asphalt were roughly 16 °C and over gravel were 17 °C. Throughout the asphalt measurements, the surface of the asphalt

was dry. The soil below the grass was damp but not saturated. The gravel was saturated; pools of standing water were in the vicinity of the measurement area. Reference 2 contains further information regarding the experimental configuration.

3. Results and Analysis

Template spectra that appear in the following analysis are obtained by calculating the spherical wave reflection coefficient with either a one-parameter or a two-parameter model inserted to describe the impedance of the ground. The one-parameter model, attributed to Delany and Bazley (*10*), is an empirically derived model for the impedance of hard-backed thin layers of absorbing materials. When normalized by the density of air and the speed of sound in air (ρ_0 and c_0 at 20 °C and 1 atm, respectively), the one-parameter model appears in the Template Method, separated into its real and imaginary parts, as

$$\text{Re}(Z_s / \rho_0 c_0) = 1 + 9.08(1000 f / \sigma_{eff})^{-0.75}$$
$$\text{Im}(Z_s / \rho_0 c_0) = 11.9(1000 f / \sigma_{eff})^{-0.73} \quad , \tag{1}$$

where *f* is the frequency in Hz, and σ_{eff} represents the effective flow resistivity of the ground in Pa·s/m^2 (*5, 10*). A second model, using two adjustable parameters to describe the impedance of the ground is attributed to Attenborough (*11*). The specific acoustic impedance ratio described by the two-parameter model appears in the Template Method, again after separation into real and imaginary parts, as

$$\text{Re}(Zs / \rho_0 c_0) = \frac{1}{\sqrt{\pi \gamma \rho_0}} \sqrt{\frac{\sigma_e}{f}}$$
$$\text{Im}(Zs / \rho_0 c_0) = \frac{1}{\sqrt{\pi \gamma \rho_0}} \sqrt{\frac{\sigma_e}{f}} + \frac{c_0 \alpha_e}{8 \pi f} \quad , \tag{2}$$

where, γ is the ratio of specific heats in air, σ_e represents the effective flow resistivity of the ground in Pa·s/m^2, and α_e represents the rate of change of porosity with depth in units of m^{-1} (*5, 11*).

The following six figures present measured and calculated level differences based on the templates provided in the Template Method. Numbers beside the black curves in each template represent the value of the effective flow resistivity used in calculating the ground impedance. The effective flow resistivity is a parameter of the soil and, in all figures, has units of 10^3 Pa·s/m^2. Results over grassland appear in figures 2 and 3, where the measured level differences have been superimposed over the templates designated by ANSI S1.18-1999. Figures 4 and 5 show measured level differences over asphalt superimposed on the templates. Figures 6 and 7 depict level difference as measured on a gravel road superimposed on the templates. Even

numbered figures show measured level differences superimposed on one-parameter model templates, and odd numbered figures show the same measured level differences superimposed on two-parameter model templates. In each of the six figures, error bars of ± one standard deviation have been placed at approximately third-octave center frequencies along the measured curves. Visual comparison between the templates and the measured level differences is used as a starting place for nonlinear least squares, fitting of the ground impedance models listed in the Template Method to the measured data.
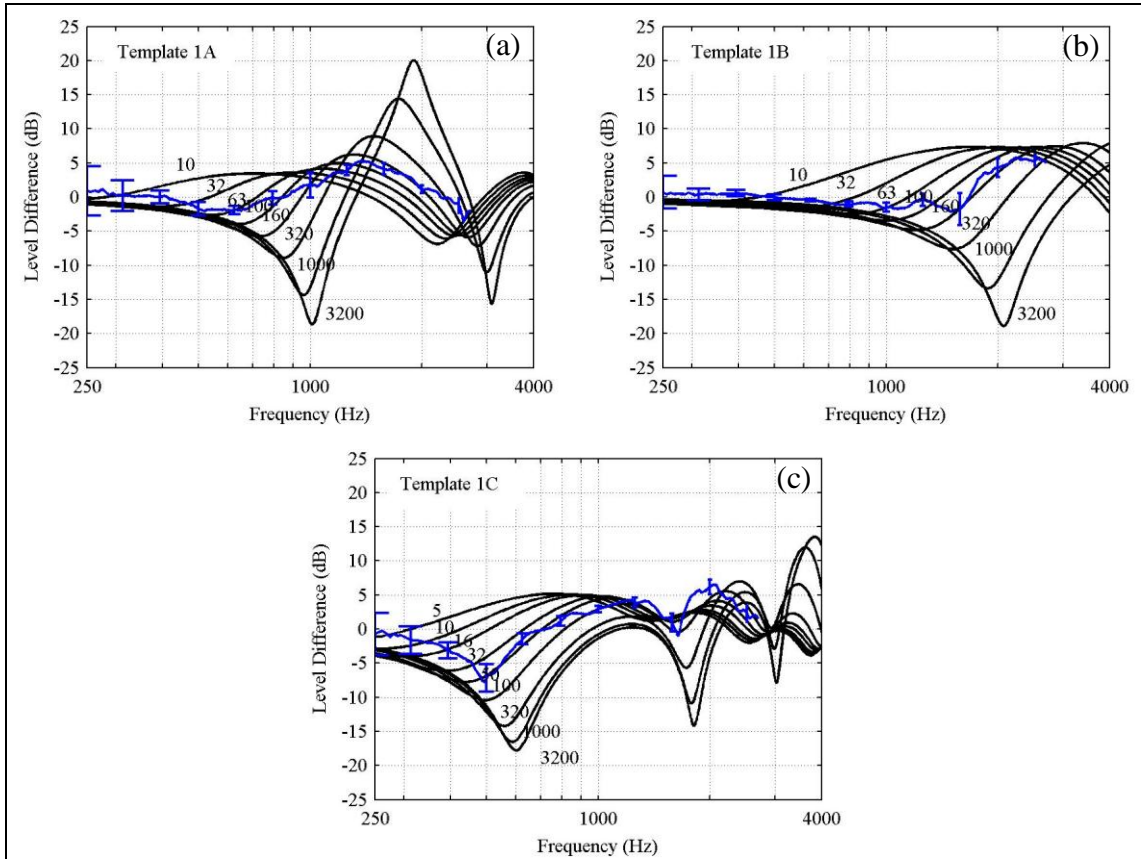

Figure 2. Grassland data (blue) superimposed over 1-parameter model templates (black).
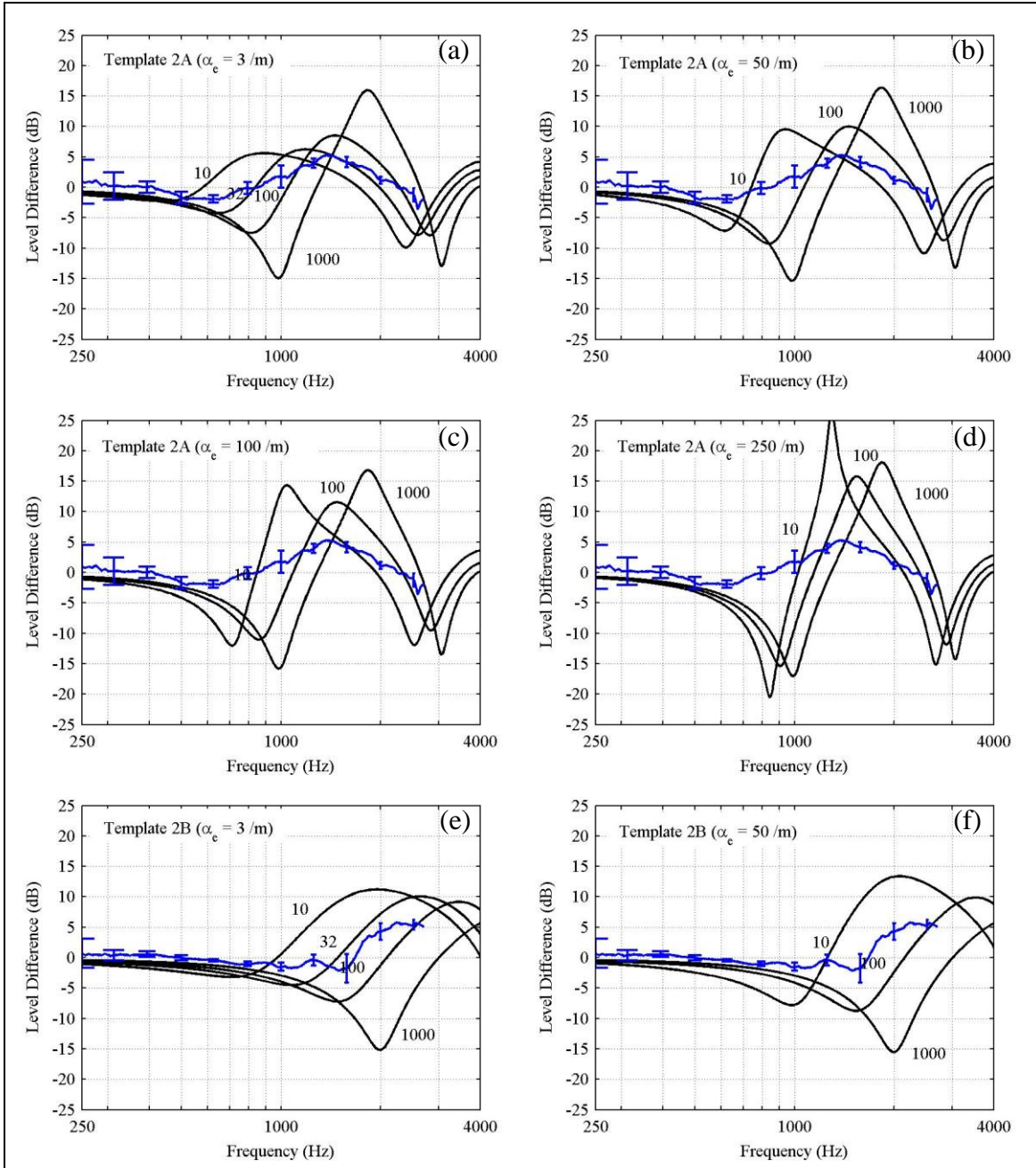
4

Figure 3. Grassland data superimposed over 2-parameter model templates (colors as in figure 2).
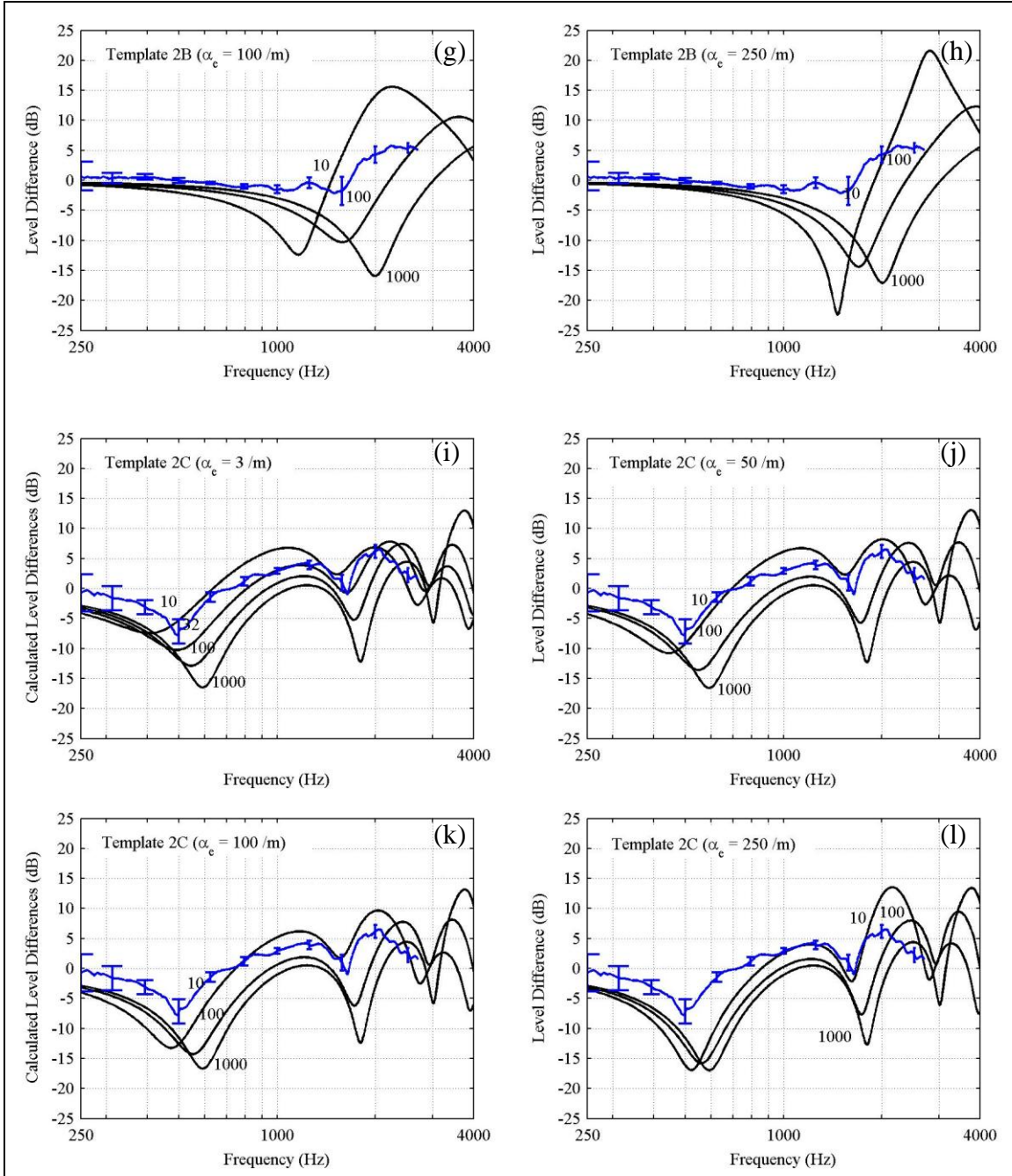
5

Figure 3. Grassland data superimposed over 2-parameter model templates (colors as in figure 2) (continued).
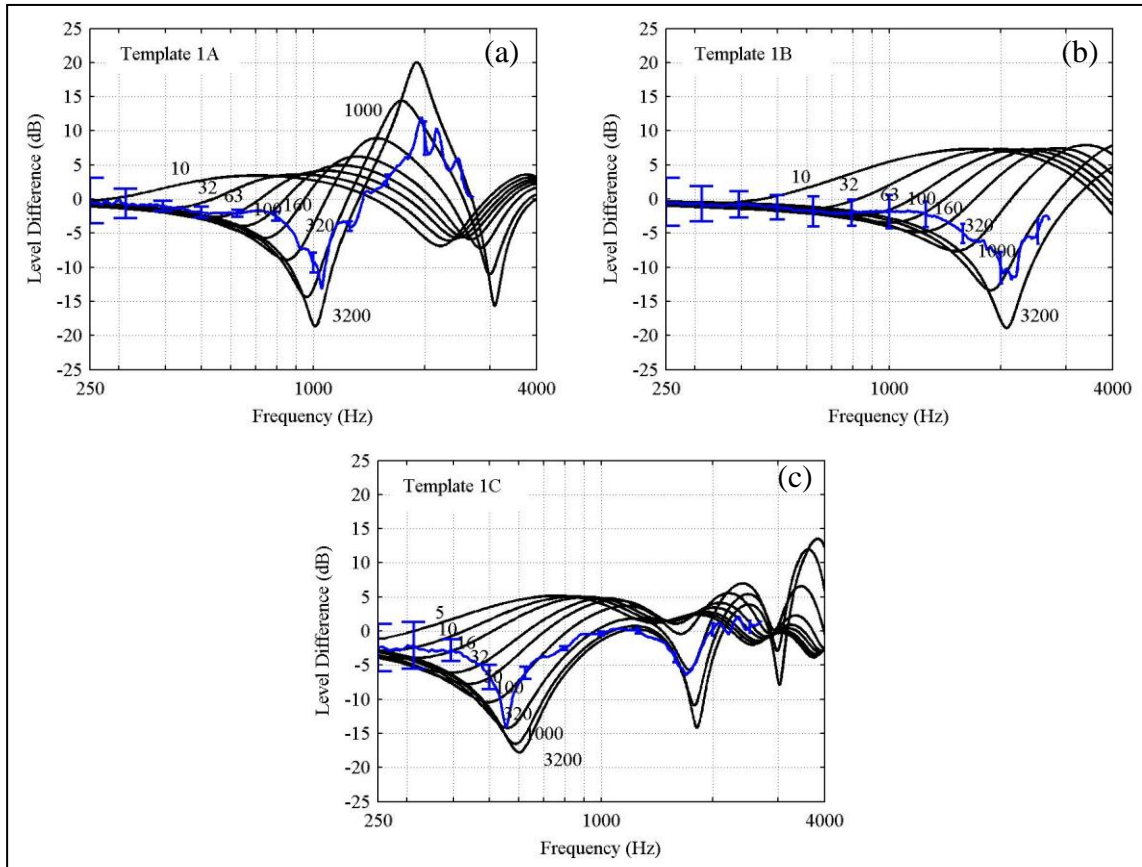
Figure 4. Asphalt road data superimposed over 1-parameter model templates (colors as in figure 2).

Figure 5. Asphalt road data superimposed over 2-parameter model templates (colors as in figure 2).

Figure 5. Asphalt road data superimposed over 2-parameter model templates (colors as in figure 2) (continued).

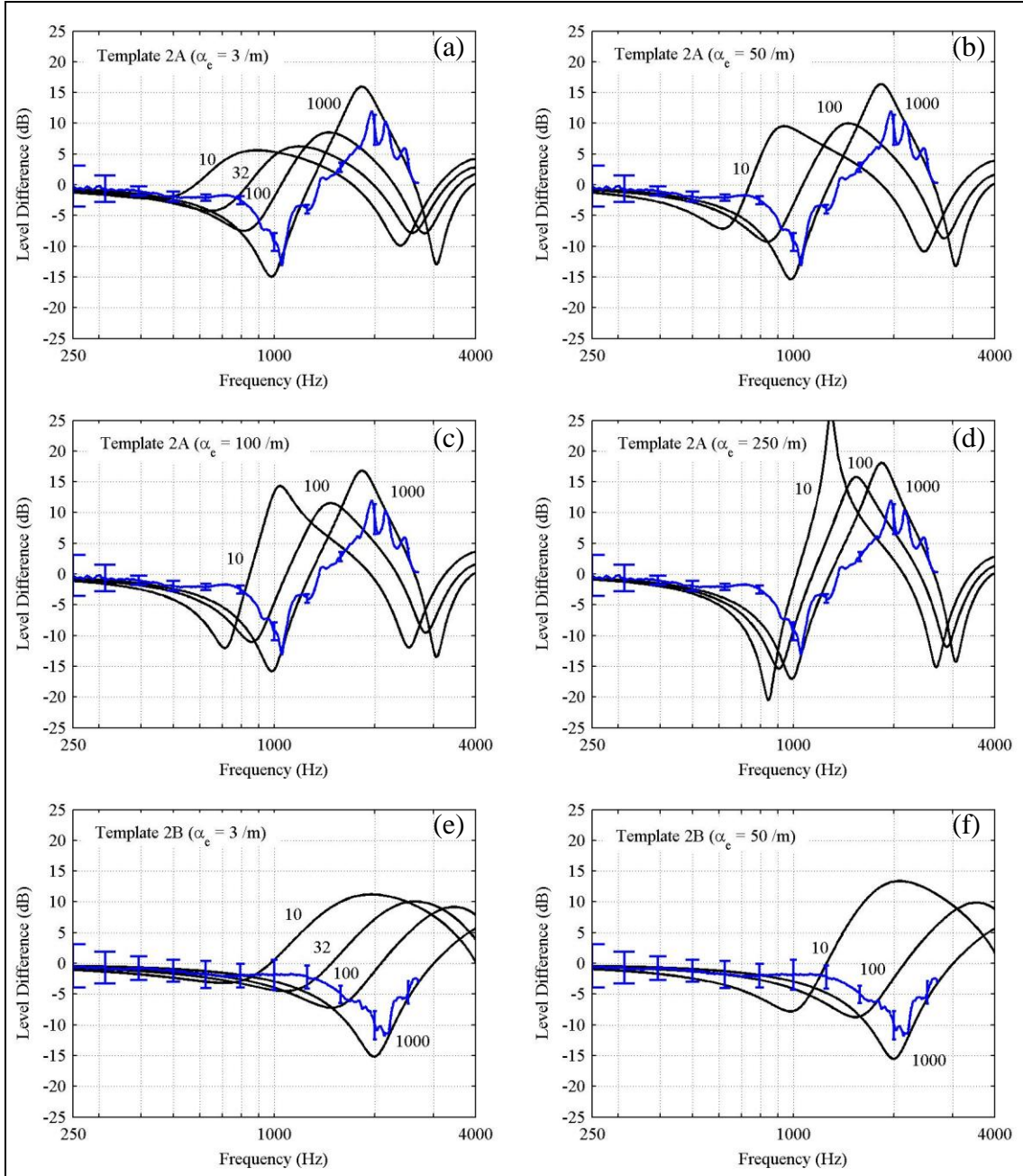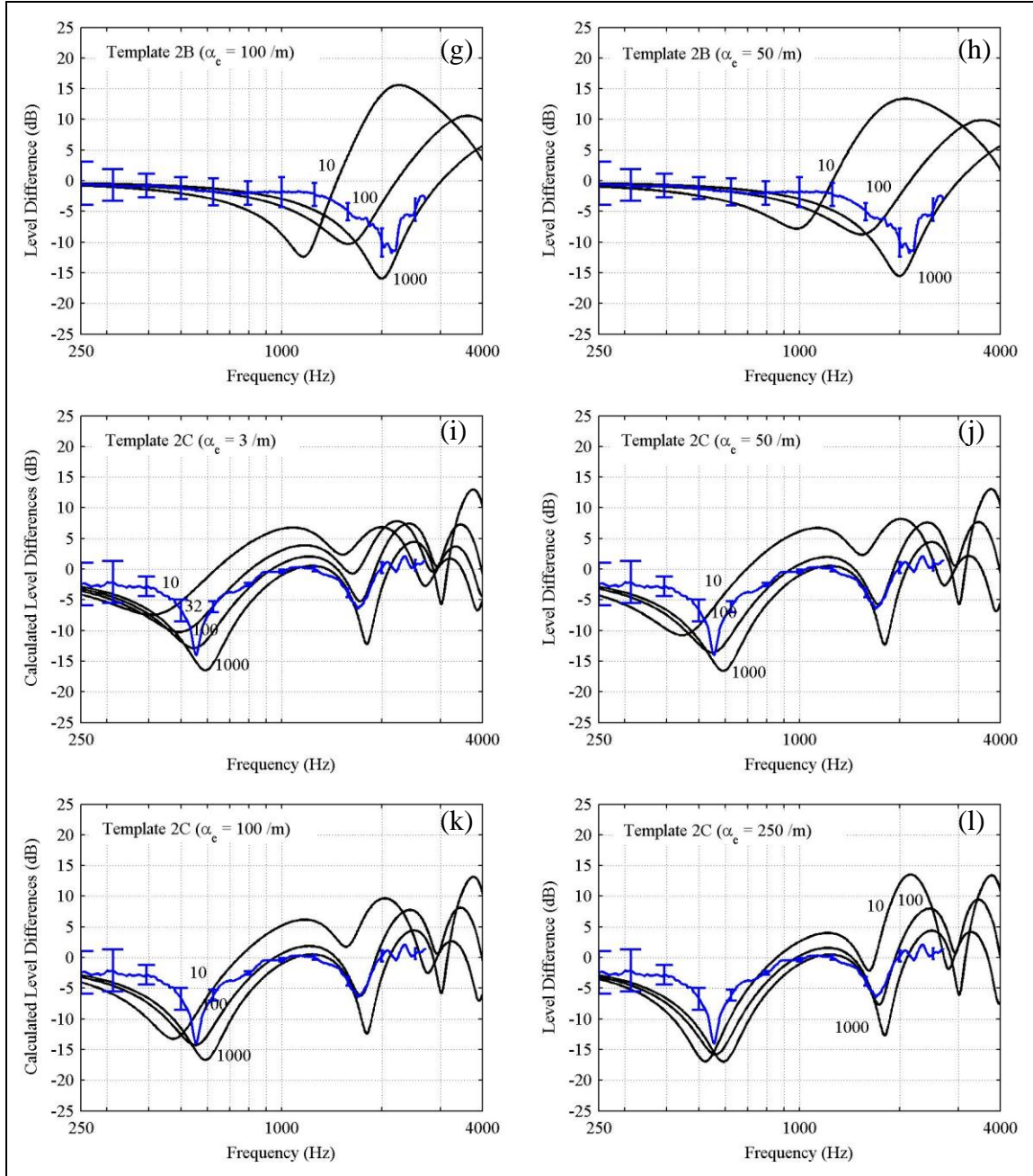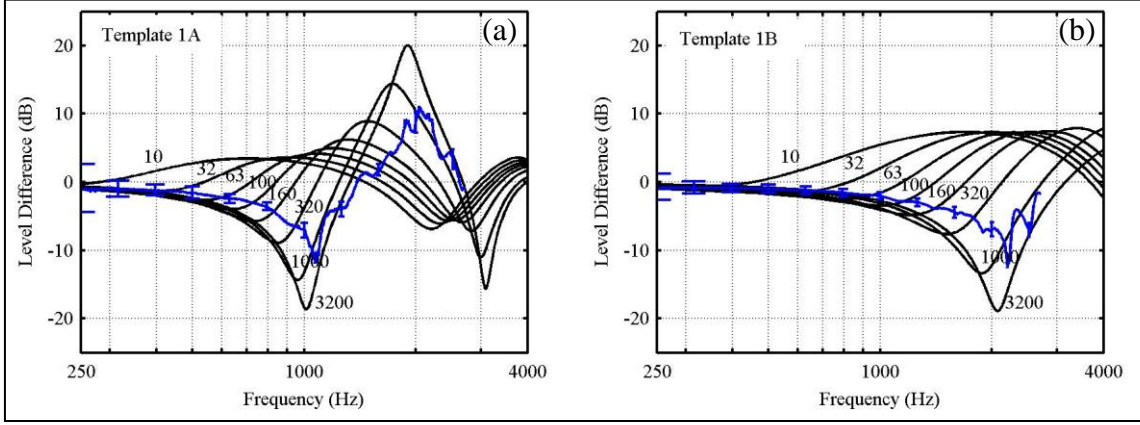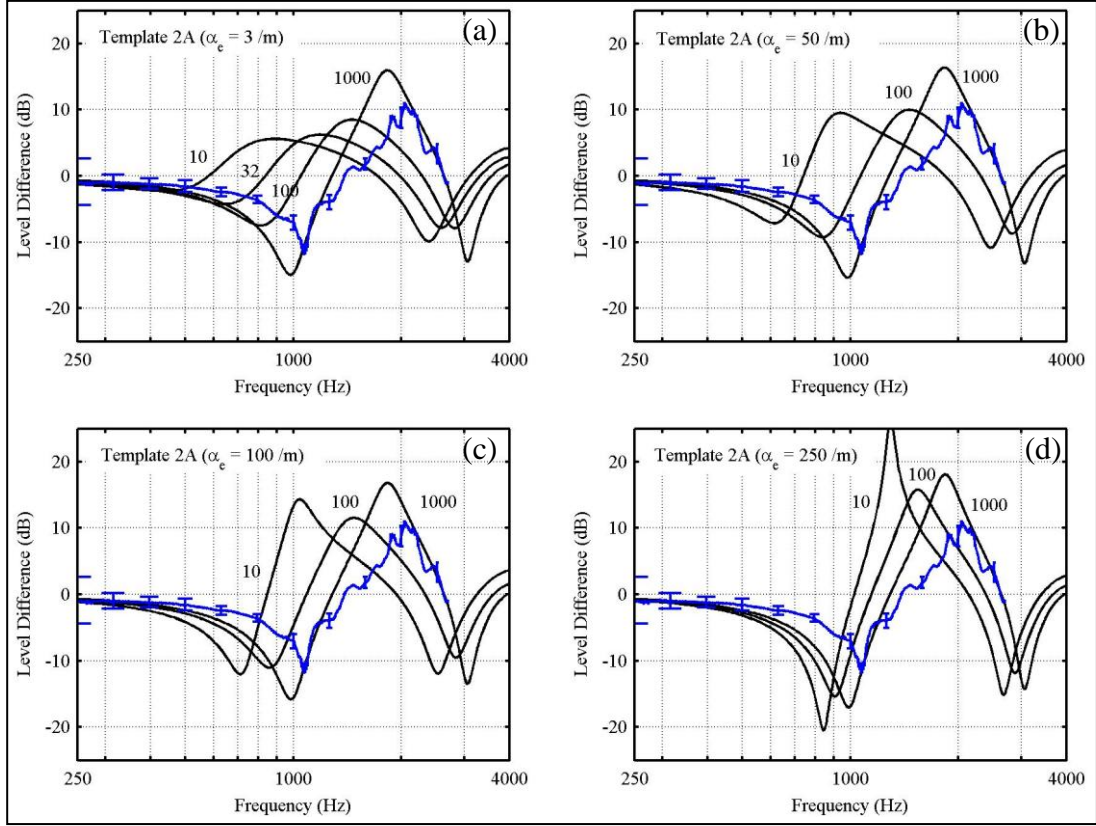Figure 6. Gravel road data superimposed over 1-parameter model templates (colors as in figure 2).

Figure 7. Gravel road data superimposed over 2-parameter model templates (colors as in figure 2).
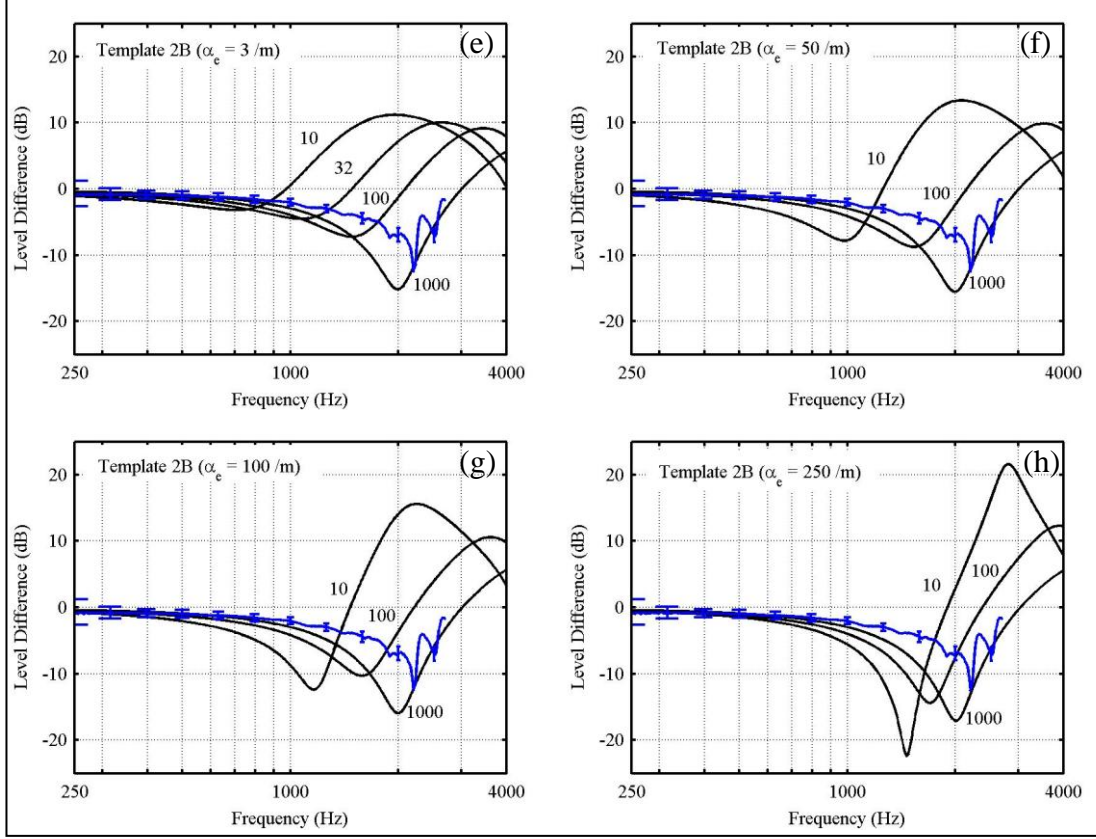
10

Figure 7. Gravel road data superimposed over 2-parameter model templates (colors as in figure 2)
(continued).

Inspection of figures 2 and 3 shows that, over grass, Templates 1C with $\sigma_{eff} = 50 \times 10^3$ Pa·s/m^2, and 2C with $\alpha_e = 3$ and $\sigma_e = 32 \times 10^3$ Pa·s/m^2, show the closest fit to the average level difference curve. The claim of closest fit is based predominantly on the frequency positions of the minima in the curve rather than on the overall fit between the measured and calculated curves. Recall that theses inspections serve as a starting place for more involved numerical fitting. Similar inspections of figures 4 and 5 show that Templates 1C with $\sigma_{eff} = 320 \times 10^3$ Pa·s/m^2, and 2C with $\sigma_e = 100 \times 10^3$ Pa·s/m^2 and for all α_e, fit well with the level difference obtained over asphalt. Repeating the procedure on the gravel level difference, as in figures 6 and 7, shows that none of the Templates exhibits a particularly good fit. These qualitative findings are reinforced if the procedures laid out in reference 5 are followed, where the cumulative errors between level differences calculated using equation 1 or 2 and measured level differences are found from the following expression:

$$E = \sum_f \left(\frac{\Delta L_c - \Delta L_a}{\sigma} \right)^2 \qquad (3)$$

In equation 3, ΔL_c is the calculated level difference, ΔL_a is an average measured level difference, and σ is the standard deviation of the averaged measurements. Note that to obtain the cumulative

error, E, the difference between the calculated and measured level differences normalized by the standard deviation of the measurement must be summed over all frequencies. In appendix A, tables A-1 and A-2 show the results of using equation 3 to compute the cumulative error between each of the one-parameter model templates and the measured level differences. Table A-3 shows the cumulative errors computed between each of the two-parameter model templates and the measured level differences. All of the cumulative errors are on the order of 10^3 or larger. This might be expected, even in cases where the calculated curves closely match the measurements, because the standard deviation of the measurements was often very small at many frequencies.

In order to obtain values for σ_{eff}, σ_e, and α_e, equations 1 and 2 were used in nonlinear least squares fitting of the measured level difference spectra (*12*). Results of the fit routines appear in figures 8 through 10, where the fit was performed over the portion of the data from 250 to 2500 Hz in an attempt to minimize potential errors at the highest frequencies due to the length of the pipe. In each of the figures, measurements are in blue with error bars at approximate third-octave center frequencies, level difference fits based on equation 1 are in green, and level difference fits based upon equation 2 are in red. Fit values of σ_{eff} in equation 1, and σ_e and α_e in equation 2, are shown in green and red, respectively. Cumulative errors, calculated by equation 3, due to each fit are shown in the same colors. It should be noted that the 1-parameter level difference fit to level difference curves, using all geometries, over gravel and asphalt are particularly poor (figures 9 and 10). Further, the large negative values of α_e—on the order of 10^3 1/m—tend to make the two-parameter fit suspect even though the curves appear to agree well with the measurements. This difficulty in fitting calculated level differences to measured level differences over such acoustically hard surfaces as asphalt and gravel is not unexpected. The application of the Template Method to these surfaces is not valid, as their impedances approach the upper limit of either impedance model. Thus, asphalt and gravel, in the case of BPRF, should be considered rigid. The one- and two-parameter fits to the level differences over grass, however, are much more reasonable (figures 8a through 8c). While the cumulative errors are large in the comparison to templates, values for σ_{eff} and σ_e are reasonable when compared to ranges listed in appendix B of the Template Method, where σ_{eff} can range from 40–300 $\times 10^3$ Pa·s/m^2, and σ_e can range from 30–400 $\times 10^3$ Pa·s/m^2 for various grass covered surfaces with varying moisture content (*5*). The negative values of α_e are unexpected, but are reasonable considering that BPRF is part of the floodplain of the Potomac River and the Nanjemoy Creek. Thus, the soil may have a large concentration of river silt. That silt content, coupled with the regular mowing of the grassland where the measurement occurred and the aerated top layer (due to root growth), could lead to a more porous layer above a lower less porous layer.
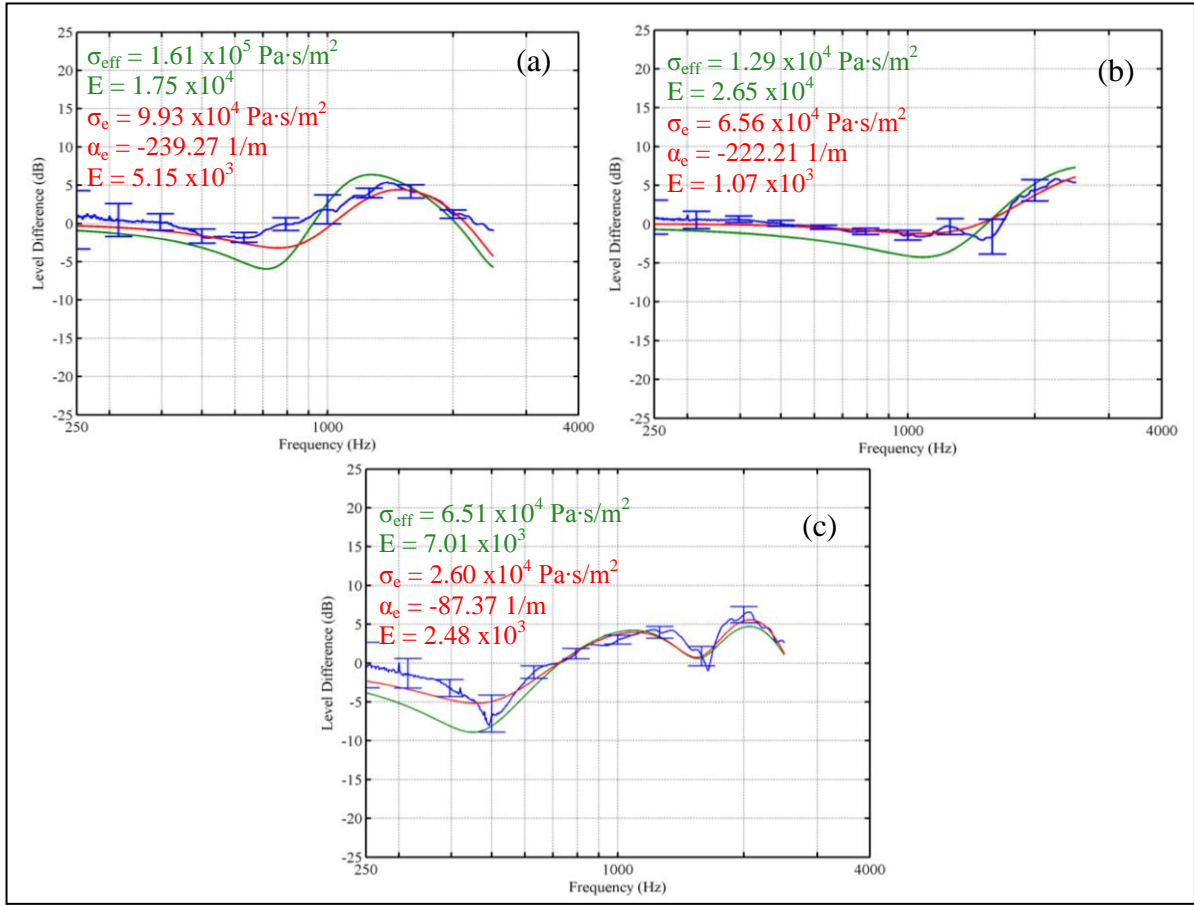
Figure 8. Non-linear least squares fit to level differences measured over grassland (blue) using one- (green) and two-parameter (red) ground impedance models. Geometry A is (a), geometry B is (b), and geometry C is (c). Fit parameters and cumulative errors are shown in the same colors as their respective models.
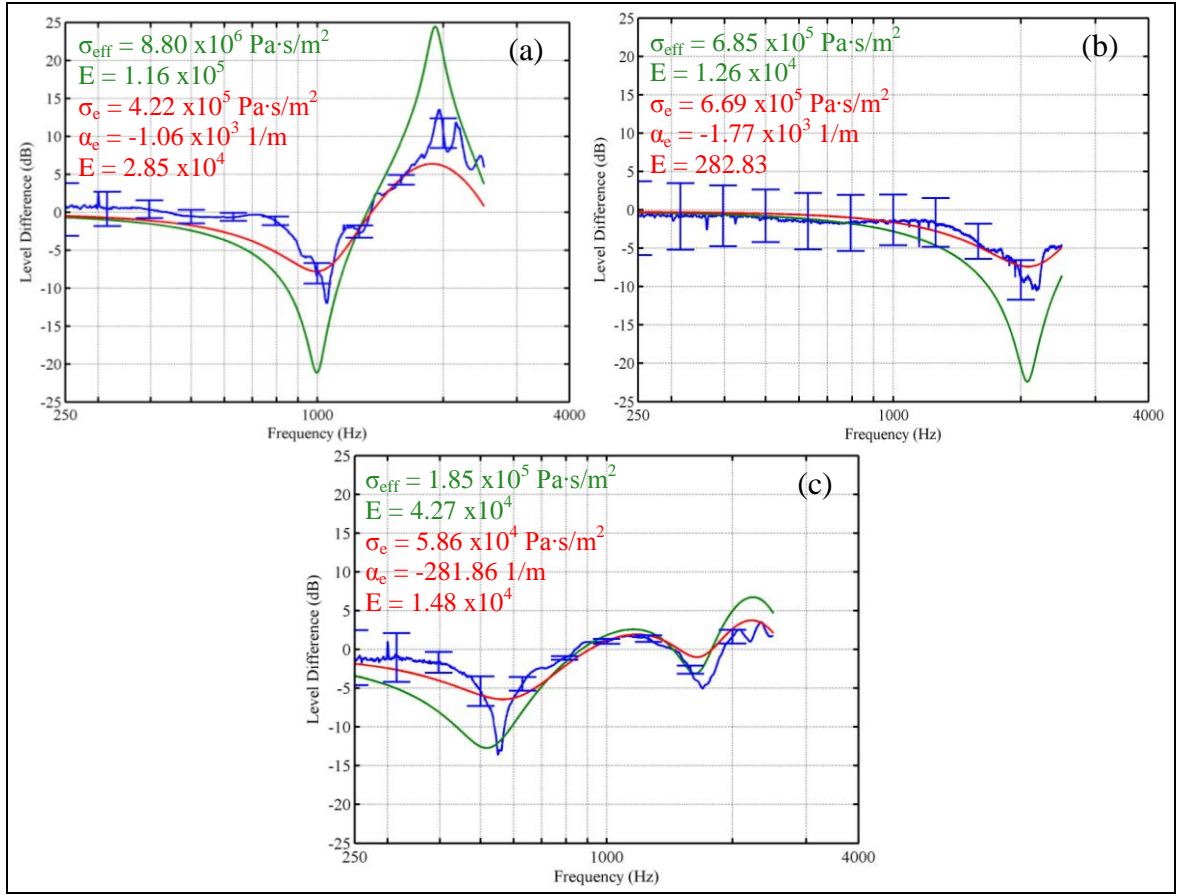
Figure 9. Non-linear least squares fit to level differences measured over asphalt using one- and two-parameter ground impedance models. Color and geometry representations are the same as in figure 8.
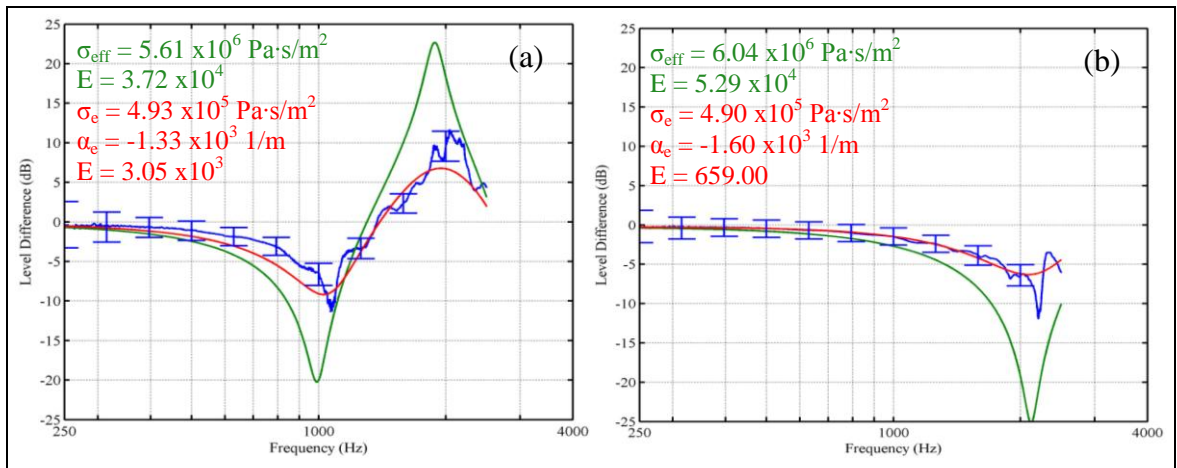

Figure 10. Non-linear least squares fit to level differences measured over gravel using one- and two-parameter ground impedance models. Geometry A is (a) and geometry B is (b). Color representations are the same as in figure 8.

14

4. Conclusions

As part of a study of sound propagation in the vicinity of an isolated building, the acoustic ground impedances of several surfaces—grass, asphalt, and gravel road—at BPRF have been deduced from measurements of level difference spectra. These spectra were measured using the procedures put forth in ANSI *S1.18-1999: Template Method for Ground Impedance*. The flow resistivity values obtained for the grass surface agree with published results, while rate of change of porosity with depth, α_e, tends to be much lower than that reported in the Template Method. The negative values of α_e are likely explained by the soil composition at BPRF. Future acoustic research at BPRF should treat the parameters reported herein as a guide only. Ground impedance can vary significantly from site to site, and can vary significantly according to the meteorological and soil conditions present at the time of the measurement.

5. References

1. Attenborough, K.; Taherzadeh, S.; Bass, H. E.; Di, X.; Raspet, R.; Becker, G. R.; Gudesen, A.; Chrestman, A.; Daigle, G. A.; L'Esperance, A.; Gabillet, Y.; Gilbert, K. E.; Li, Y. L.; White, M. J.; Naz, P.; Noble, J. M.; van Hoof, H.A.J.M. Benchmark Cases for Outdoor Sound Propagation Models. *J. Acoust. Soc. Am.* **1995**, *97* (1), 173–191.

2. Albert, D. G. Acoustic Waveform Inversion with Application to Seasonal Snow Covers. *J. Acoust. Soc. Am.* **2001**, *109* (1), 91–101.

3. Sabatier, J. M.; Hess, H.; Arnott, W. P.; Attenborough, K.; Romkens, M.J.M.; Grissinger, E. H. In Situ Measurements of Soil Physical Properties by Acoustical Techniques. *Soil Sci. Soc. Am. J.* **1990**, *54*, 658–672.

4. Alberts, W.C.K. II; Noble, J. M.; Coleman, M. A. Sound Propagation in the Vicinity of an Isolated Building: An Experimental Investigation. *J. Acoust. Soc. Am.* **2008**, *124* (2), 733–742 ().

5. *S1.18-1999: Template Method for Ground Impedance*; American National Standards Institute, 1999.

6. Don, C. G.; Cramond, A. J. Soil Impedance Measurements by an Acoustic Pulse Technique. *J. Acoust. Soc. Am.* **1985**, *77* (4), 1601–1609.

7. Sabatier, J. M.; Raspet, R.; Frederickson, C. An Improved Procedure for the Determination of Ground Parameters Using Level Difference Measurements. *J. Acoust. Soc. Am* **1993**, *94* (1), 396–399.

8. Zuckerwar, A. J. Acoustic Ground Impedance Meter. *J. Acoust. Soc. Am.* **1983**, *73* (6), 2180–2186.

9. Williams, J. *An Acoustic Ground Impedance Measurement*; ARL-TN-221; U.S. Army Research Laboratory: White Sands Missile Range, NM, July 2004.

10. Delany, M. E.; Bazley, E. N. Acoustical Properties of Fibrous Absorbent Materials. *Appl. Acoust.* **1970**, *3*, 105–116.

11. Attenborough, K. Ground Parameter Information for Propagation Modeling. *J. Acoust. Soc. Am.* **1992**, *92* (1), 418–427.

12. Press, W. H.; Flannery, B. P.; Teukolsky, S. A.; Vetterling, W. T. *Numerical Recipes in C: The Art of Scientific Computing*; Cambridge University Press: New York, 1988.

Appendix A. Tables of Cumulative Errors

Tables in this appendix list the cumulative errors obtained from using equation 3 when comparing measurements to the templates.

Table A1. Cumulative errors between the measurements and templates for the one-parameter model and geometries A and B.

Surface	Geometry	σ_{eff} (10³ Pa·s/m²)								
		10	32	63	100	160	320	1000	3200	10000
Grass	A	6182	5844	5661	5568	5496	5424	5360	5332	5320
Grass	B	6596	6310	6199	6146	6108	6070	6038	6024	6019
Asphalt	A	8525	8437	8396	8378	8365	8353	8344	8340	8338
Asphalt	B	2603	2742	2805	2837	2862	2888	2910	2920	2924
Gravel	A	22784	22523	22390	22324	22275	22226	22185	22166	22159
Gravel	B	15651	16697	17184	17434	17627	17825	18001	18080	18113

Table A2. Cumulative errors between the measurements and templates for the one-parameter model for geometry C.

Surface	Geometry	σ_{eff} (10³ Pa·s/m²)								
		5	10	16	32	50	100	320	1000	3200
Grass	C	15506	15393	14895	14094	13661	13162	12691	12484	12393
Asphalt	C	5768	5710	5463	5107	4938	4763	4621	4566	4543

Table A3. Cumulative errors between the measurements and templates for the two-parameter model for all geometries specified in Table 1. Units of σ_e are 10³ Pa·s/m².

Surface	Geom.	$\alpha_e = 3$ m⁻¹				$\alpha_e = 50$ m⁻¹			$\alpha_e = 100$ m⁻¹			$\alpha_e = 250$ m⁻¹		
	σ_e	10	32	100	1000	10	100	1000	10	100	1000	10	100	1000
Grass	A	5913	5638	5493	5368	5854	5499	5369	5718	5490	5370	5527	5450	5368
Grass	B	6353	6189	6109	6043	6288	6108	6043	6211	6101	6043	6115	6079	6042
Grass	C	14326	13404	12924	12512	14049	12933	12515	13603	12899	12516	13001	12763	12510
Asphalt	A	8453	8392	8365	8345	8439	8366	8345	8408	8364	8345	8371	8357	8345
Asphalt	B	2719	2811	2862	2907	2754	2862	2906	2798	2866	2906	2858	2881	2907
Asphalt	C	5205	4845	4689	4573	5089	4691	4574	4916	4681	4574	4712	4641	4572
Gravel	A	22190	17981	22190	17981	22190	17981	22190	17981	22190	17981	22190	17981	22190
Gravel	B	22244	17775	22244	17775	22244	17775	22244	17775	22244	17775	22244	17775	22244